The Holocene East Asian–Australian summer monsoon: A see-saw relationship

Deniz Eroglu,[1,2*] Fiona H. McRobie,[3] Ibrahim Ozken,[1,4] Thomas Stemler,[5]

Karl-Heinz Wyrwoll,[3] Norbert Marwan,[1] Jürgen Kurths[1,2,6]

[1] *Potsdam Institute for Climate Impact Research (PIK), 14473 Potsdam, Germany*

[2] *Department of Physics, Humboldt University, 12489 Berlin, Germany*

[3] *School of Earth and Environment, The University of Western Australia, Crawley, Western Australia 6009, Australia*

[4] *Department of Physics, Ege University, 35100 Izmir, Turkey*

[5] *School of Mathematics and Statistics, The University of Western Australia, Crawley, Western Australia 6009, Australia*

[6] *Institute for Complex Systems and Mathematical Biology, University of Aberdeen, Aberdeen AB24 3UE, United Kingdom*

The East Asian–Indonesian–Australian monsoon (EAIAM) regime is the largest low–latitude monsoon system. It links the Earth's hemispheres, providing a planetary–scale heat source that drives the global circulation during boreal winter [1]. At both seasonal and inter–seasonal time scales, the summer monsoon of one hemisphere is linked via outflows from the winter monsoon of the opposing hemisphere [2]. Over longer times, likely phase relationships between the East Asian summer monsoon (EASM) and Indonesian–Australian summer monsoon (IASM) are only beginning to be understood [3–6]. With this uncertainty come questions of likely long–term adjustments to future greenhouse–triggered climate change, and whether these changes could 'lock–in' possible phase relationships between the IASM and EASM regimes in a region where billions of people's lives depend highly on monsoon–related rainfall. Here we show that our newly–developed non–linear time series analysis technique [7] enables us to confidently identify monsoon regime changes at millennial to sub–centennial time scales and identify a see–saw relationship over some 9000 years – with wet and dry monsoon states essentially

opposingly phased. Our results provide a step towards a better understanding of the centennial– to millennial–scale relationships within the EAIAM regime.

We use the high resolution speleothem paleoproxy records of KNI-51 ($15.30°$S, $128.61°$E) from northwestern Australia and Dongge Cave ($25.28°$N, $108.08°$E) from southern China (Fig.1) to outline the summer monsoon states of the last c. 9000 years. The details of the U/Th chronology and associated stable isotope records are provided by Denniston et al. [5] and Wang et al. [9] respectively. Both caves are well placed to capture the respective summer monsoon regimes located at the end points of the broader EAIAM system (Fig. 1 and Supp. Mat.).

The records of Dongge Cave and KNI-51, as with many paleoclimate proxy records, are irregularly sampled, i.e.: the time between two consecutive measurements is not constant and may vary largely along the length of the record. Most time series analysis methods, however, require regular sampling. Traditionally, some form of interpolation is used to deal with these irregularities, but this introduces additional information into the time series with much higher uncertainty than the real observations [10]. To avoid corrupting the quality of the speleothem proxy records, we developed a new method (for details, see [7,11]) based on techniques used for neurological data [12]. This method, the Transformation Cost Time Series (TACTS) method, produces a regularly sampled time series and allows us to identify regime changes using standard time series analysis.

[Figure 1 about here.]

In essence, the TACTS method determines the 'cost' of transforming one segment of the record into the following segment. For this transformation we allow three possible modifications: (i) changing the amplitude of a data point, (ii) shifting a data point in time, and (iii) creating or deleting a data point. The 'cost' for changing the amplitude and shifting a data point is linearly dependent on the size of the modification. On the other hand, creating and deleting data points should be 'expensive' enough to not favour this modification over the other two points (see Supp. Mat. for an illustration of this method). The resulting time series is regularly sampled, and we analyse it using recurrence plot analysis and derive the determinism. This is a measure of predictability, and is therefore well suited to detect regime

changes in the time series [13] (see Supp. Mat. for details).

[Figure 2 about here.]

Our analysis of the Dongge Cave and KNI-51 records reveals alternating periods of statistically significant strong/weak monsoon states of centennial to millennial durations (Fig. 2). The shaded bands in the figure depict 90% confidence intervals (see Supp. Mat.), with wet/dry states defined as exceeding these bands. Prolonged wet/dry states are recognised, and the comparison given by the coloured bands in Fig. 2 highlights that our quantitative technique is able to reveal new details of the monsoon dynamics.

The wet/dry regimes identified improve upon previous, qualitative interpretations of the proxy records [5,9,14]. Here we provide a detailed discussion of where our method supports, corrects and improves the analysis and interpretation of previous studies. We particularly focus on regimes which are newly identified or previously incorrectly interpreted.

In the KNI-51 record (north west Australian summer monsoon) the major wet (dry) phases occur between 8.5-6.4 ka, (6.3-5.0 ka), 5.0-4.0 ka, possibly extending to 3.0 ka, (3.0-1.4 ka), 1.3-0.9 ka, with a transition at 0.9 ka to the present monsoon regime. Embedded within these time intervals are additional events of centennial to sub–centennial duration. The major phase differences of our analysis show some correspondence with inferences drawn from a Holocene pollen/sediment record of monsoon events [15], but our analyses offer improved time resolution and greater details of the inherent variability within major monsoon phases.

The Dongge Cave monsoon record has been discussed in detail by Wang et al. [9] and further developed by Hu et al. [14]. Wang et al. [9] recognised eight weak monsoon events lasting 100 to 500 years: at 0.5 ka, 1.6 ka, 2.7 ka, 4.4 ka, 5.5 ka, 6.3 ka, 7.2 ka and 8.3 ka. While adding some details, the Hu et al. [14] reconstructions essentially concur with those of Wang et al. [9]. Our results indicate wet (dry) regime intervals between (8.2-7.6 ka), 7.6-7.2 ka, (7.1-6.9 ka), (6.4-5.8 ka), 5.8-5.0 ka, (5.0-4.0 ka), 3.0-2.7 ka, (2.2-2.0 ka), 1.9-0.8 ka and (0.7-0.4 ka).

Our analysis has revealed details for KNI-51 and Dongge Cave not previously recognised (Fig.2). In the KNI-51 record two events, absent from Denniston et al. [5], occur at 6.6-6.4 ka (wet) and 7.0-6.8 ka (dry). Furthermore, our results improve upon the findings of Denniston et al. [5] and McGowan et al. [15] by reclassifying previously misinterpreted regimes. We identify a wet regime at 3.2-3.1 ka (wet) previously interpreted as dry [15] and similarly a dry regime at 7.6-7.5 ka incorrectly claimed to be wet by Denniston et al. [5]. Similarly, the results of our Dongge Cave analysis contradict the conclusions of Hu et al. [14] for the time periods 6.2-6.1 ka (dry) and 7.8-7.6 ka (dry). In addition, there are three events identified by Hu et al. that are not statistically significant in our analysis (3.4-3.2 ka, 6.9-6.3 ka and 8.8-8.2 ka). We assert confidence in these revisions, as they are based on a rigorous, quantitative analysis, rather than rudimentary visual comparison of data sets.

Moreover, our results reveal a striking wet–dry, opposing relationship between the IASM [5] and EASM [9] (Fig. 2). The only time when this see–saw relationship is not observed is during 7.6-7.2 ka, when both monsoon records show a 'wet state'. Over the entire time scale, the cross–correlation of the determinism time series is -0.27, and while this affirms an antiphased relationship, it does not capture the strong correspondence between the statistically significant wet/dry monsoon states. In fact the antiphased relationship is much stronger, if only the statistical significant parts of the time series are used and the internal variability on sub–centennial to decadal time scales is ignored. This may be calculated using a step function filter, yielding a cross–correlation of -0.33. Therefore the variability at sub–centennial to decadal time scales in both the Dongge Cave and KNI-51 records is emphasised; such short–term variability is evident in present day monsoon records from both regions [16].

While the details of the controls and processes determining the function and latitudinal extent of the respective summer monsoons are more complex [1, 2] than simply relating them to the position of the Intertropical Convergence Zone (ITCZ), the ITCZ provides a convenient metric of monsoon extent [1, 17]. For the broader EAIAM history, the displacement of the ITCZ is a driver that has been advocated in a range of Quaternary paleoclimate studies [18–21]. The argument recognises that the ITCZ is displaced towards the warmer hemisphere in response to differential cooling [22–24]. This is an attractive and apparently straightforward explanation, with a caveat that the ITCZ over

the region of the West Pacific Warm Pool (i.e. the Maritime Continent) is much less well defined than over the wider Pacific and Indian Oceans, with a more complex south–north (north–south) seasonal migration pattern [17, 25, 26].

In explaining the Dongge Cave δ^{18}O record, Wang et al. [9] appeal to a likely displacement of the ITCZ driven by solar variability. Their basis for this claim is the use of the atmospheric Δ^{14}C record as a proxy for solar activity, with which they obtain a correlation of 0.3 with their speleothem δ^{18}O record. We extend this claim further and ask whether the Holocene antiphase relationship that we have uncovered in the summer monsoons of the overall EAIAM is driven by solar variability.

To establish this, we compare the determinism–measure of solar activity with that derived from the EASM and IASM proxy records. The analysis identifies a statistically significant correlation (see Supp. Mat. for details) between solar activity and both records from Dongge Cave (0.29) and KNI-51 (-0.32). Thus, when predictability of solar activity is high (low), the Dongge Cave record indicates a strong (weak) summer monsoon, while northern Australia experiences a weak (strong) summer monsoon. Increased predictability of solar activity corresponds to periods of a consistently high number of solar 'events', increasing the solar irradiance received by the Earth. Positive correlation with the Dongge Cave record therefore indicates a direct control, whereby periods of increased solar activity enhance the summer monsoon over East Asia. The asymmetric response in the Australian monsoon record suggests that periods of increased solar irradiance actually decrease monsoon strength. To explain this, we consider orbital–scale positioning of the ITCZ. Preferential heating of the Northern Hemisphere during periods of high tilt and Northern Hemisphere perihelion, as observed from 9-3 ka, provides a background driver for increased EASM strengthening. At a global scale, there is a northward shift in the ITCZ, weakening monsoon activity over north west Australia. Coupling this with solar activity, brief periods of increased irradiance would act to shift the ITCZ further north, and we would therefore expect a stronger EASM and corresponding weak IASM. This model is supported by our analysis, and compounded by the observation that from c.2.5 ka onwards, as orbital controls begin to favour the Southern Hemisphere, correspondence between the determinism–measure of solar activity and EASM and IASM records diminishes. These findings lead us to conclude that solar activity provides a driver in the see–saw relationship

observed between the EASM and IASM over the past 9000 years, modulated by orbital–scale ITCZ positioning.

A significant body of work is now available that proposes the impact of solar variability on the tropical atmosphere [27–30]. This work demonstrates that the Hadley and Walker circulation cells are affected by solar variability, and through this, trigger an increase in tropical precipitation during periods of high solar activity and an associated change in the position of the ITCZ. We demonstrate that solar variability can impact summer monsoon strength, and more importantly provides the control of the antiphase relationship between the EASM and IASM over the last 9000 years. Our results reveal a strong coupling between the monsoons of the two hemispheres, expressed as a see–saw relationship, and driven by decadal– to centennial–scale variations in solar activity.

Methods

To calculate the transformation cost time series we determine the cost for transformation of one segment into another for two successive segments of a time series. Treating each observation as an 'event', we seek to transform the events in the first segment into those of the second. For a single transformation, this cost is a generalised distance between these two segments. Therefore, as a distance, the cost must be a positive number, symmetrical (i.e. transforming the first into the second is the same as transforming the second into the first), and must satisfy the triangle inequality.

The cost associated with each transformation is given by:

$$\begin{aligned} p(c) = \quad & \textstyle\sum_{(\alpha,\beta)\in C} \quad \{\lambda_0 |t_a(\alpha) - t_b(\beta)| + \\ & \tfrac{1}{m}\textstyle\sum_{k=1}^{m} \quad \lambda_k |L_{a,k}(\alpha) - L_{b,k}(\beta)|\} + \\ & \lambda_S(|I| + |J| - 2|C|), \end{aligned} \tag{1}$$

where I and J are a set of indices of the events in starting set S_a and the final set S_b, respectively. These sets – S_a and S_b – correspond to the events in the two time series segments. The first summation quantifies the cost associated with shifting events in time. We sum over the pairs $(\alpha, \beta) \in C$, where the set C comprises the points that need to

be shifted in time. α and β denote the αth event in S_a and βth event in S_b. The coefficient λ_0 is the cost factor for time shifts. The second summation calculates the cost due to changing the amplitude of events. This involves the difference $|L_{a,k}(\alpha) - L_{b,k}(\beta)|$, where $L_{a,k}(\alpha)$ is the amplitude of the αth event in S_a. The parameter λ_k has the unit of amplitude^{-1} and the sum is over the different components of the amplitude. That is, if we are dealing with one dimensional data $m = 1$, while for a three dimensional phase space m would be three. The last terms in the cost function deal with the events not in C which have to be added or deleted. Note that $|\cdot|$ denotes the size of the set and λ_S is the cost parameter for this operation. Suzuki *et al.* omitted this parameter, since they chose a cost of one for such an operation [11].

We determine the cost factors λ_0, λ_k based on the time series at hand:

$$\lambda_0 = \frac{M}{\text{total time}} \tag{2a}$$

$$\lambda_k = \frac{M-1}{\sum_i^{M-1} |L_a - L_b|}, \tag{2b}$$

where M is the total number of events in the time series. Note that λ_0 is the mean event frequency and λ_k is the inverse of the average amplitude difference.

The cost factor λ_S is an optimisation parameter. We constrain $\lambda_S \in [0, 4]$ and explore the costs of deleting or adding an event to our time series. If our time series consists of $n + 1$ segments of equal length, we can calculate n costs for each individual transformation of the segments. Assuming that the costs are linearly independent, the central limit theorem indicates that the distribution of the costs should be a normal distribution. In particular, when dealing with non-stationary data we find that changing λ_S such that the distribution becomes normal greatly improves the skill of our time series analysis method.

For each proxy record, the detrended time series is divided into segment sizes of 20 years containing, on average, 4 to 5 points. The final results shown in Fig. 2 are relatively insensitive to the choice of segment size. The proportionality parameters for modifications (i) and (ii) are determined from the proxy records and are related to the average amplitude and sampling time. The creation and deletion cost factor λ is our optimisation parameter, chosen

relative to the other parameters. Determining the costs of transformation provides a measure of how close one segment is to the following one and produces a regularly sampled transformation cost time series with a temporal resolution of 20 years. Using recurrence plot analysis we are able to quantify the predictability of each segment by deriving the determinism [13]. Abrupt transitions into or out of a 'wet' or 'dry' state are hard to predict, while behaviour within a regime follows a somewhat similar pattern throughout. As a result, determinism is particularly effective at identifying regime changes (see Supp. Mat. for further details).

Acknowledgement

DE and NM acknowledge support by the Leibniz Association (WGL) under Grant No. SAW-2013-IZW-2. FM?s research is funded through an Australian Postgraduate Award. IO is financially supported from TUBITAK under 2214/A program. KHW wishes to thank Rhawn F. Denniston for his wider involvement in the northwest Australian monsoon project and the Kimberley Foundation Australia for financial support for this project and Paul Paul Wyrwoll for helpful comments.

References

[1] J. L. McBride, *Indonesia, Papua New Guinea and Tropical Australia: the Southern Hemisphere Monsoon. Meteorology of the Southern Hemisphere*, Karoly, D. J., D. G. Vincent, eds. (American Meteorological Society, Boston, 1998), pp. 89–99.

[2] C.-P. Chang, P. Harr, J. McBride, H.-H. Hsu, *East Asian Monsoon. World Scientific Series on Meteorology of East Asia, vol. 2*, C.-P. Chang, ed. (World Scientific Publishing Co. Pte. Ltd, Singapore, 2004), pp. 107–150.

[3] K. H. Wyrwoll, Z. Liu, G. Chen, J. E. Kutzbach, X. Liu, *Quaternary Science Reviews* **26**, 3043 (2007).

[4] L. K. Ayliffe, *et al.*, *Nature Communications* **4**, 2908 (2013).

[5] R. F. Denniston, *et al.*, *Quaternary Science Reviews* **78**, 155 (2013).

[6] M. Mohtadi, *et al.*, *Nature* **509**, 76 (2014).

[7] I. Ozken, *et al.*, *Phys. Rev. E* **91**, 062911 (2015).

[8] M. Kanamitsu, *et al.*, *Bulletin of the American Meteorological Society* **83**, 1631?1643 (2002).

[9] Y. Wang, *et al.*, *Science* **308**, 854 (2005).

[10] K. Rehfeld, N. Marwan, J. Heitzig, J. Kurths, *Nonlinear Processes in Geophysics* **18**, 389 (2011).

[11] S. Suzuki, Y. Hirata, K. Aihara, *International Journal of Bifurcation and Chaos* **20**, 3699 (2010).

[12] J. D. Victor, K. P. Purpura, *Network: Computation in Neural Systems* **8**, 127 (1997).

[13] N. Marwan, M. C. Romano, M. Thiel, J. Kurths, *Physics Reports* **438**, 237 (2007).

[14] C. Hu, G. M. Henderson, S. X. Junhua Huang, Y. Sun, K. R. Johnson, *Earth and Planetary Science Letters* **266**, 221 (2008).

[15] H. McGowan, S. Marx, P. Moss, A. Hammond, *Geophysical Research Letters* **39**, L22702 (2012).

[16] P. J. Webster, *The Asian Monsoon*, B. Wang, ed. (Springer Praxis Publishing, Chichester,UK, 2006), pp. 3–66.

[17] D. E. Waliser, C. Gautier, *Journal of Climate* **6**, 2162 (1993).

[18] G. Yancheva, *et al.*, *Nature* **445**, 74 (2007).

[19] M. L. Griffiths, *et al.*, *Earth and Planetary Science Letters* **292**, 27 (2010).

[20] A. N. Meckler, M. O. Clarkson, K. M. Cobb, H. Sodemann, J. F. Adkins, *Science* **336**, 1301 (2012).

[21] J. M. Russell, *et al.*, *Proceedings of the National Academy of Sciences* **111**, 5100 (2014).

[22] J. C. H. Chiang, *Paleoceanography* **18**, 1 (2003).

[23] A. J. Broccoli, K. a. Dahl, R. J. Stouffer, *Geophysical Research Letters* **33**, 1 (2006).

[24] A. Donohoe, J. Marshall, D. Ferreira, D. McGee, *Journal of Climate* **26**, 3597 (2013).

[25] C.-W. Hung, M. Yanai, *Quarterly Journal of the Royal Meteorological Society* **130**, 739 (2004).

[26] P. Xian, R. L. Miller, *Journal of the Atmospheric Sciences* **65**, 1878 (2008).

[27] H. van Loon, G. A. Meehl, J. M. Arblaster, *Journal of Atmospheric and Solar-Terrestrial Physics* **66**, 1767 (2004).

[28] D. T. Shindell, G. Faluvegi, R. Miller, G. Schmidt, J. Hansen, *Geophysical Research Letters* **33**, L24706 (2006).

[29] J. N. Lee, D. T. Shindell, S. Hameed, *Journal of Climate* **22**, 5870 (2009).

[30] G. A. Meehl, J. M. Arblaster, K. Matthes, F. Sassi, H. van Loon, *Science* **325**, 1114 (2009).

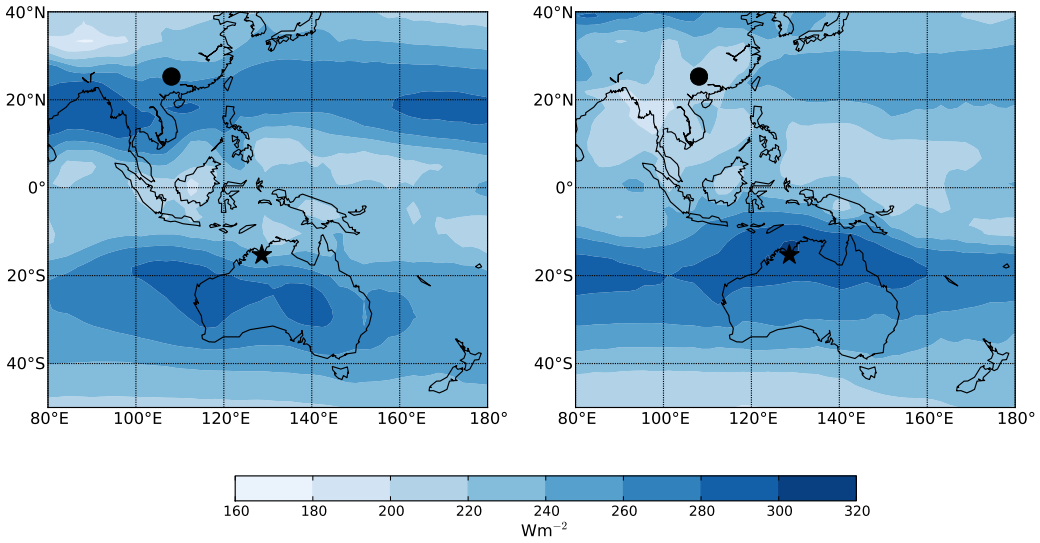

Figure 1: Top of atmosphere outgoing long wave radiation delimiting the extent of: a) East Asian summer monsoon (JJA); and b) Indonesian Australian summer monsoon (DJF) [8]. Dongge Cave (dot) and KNI-51 (star)

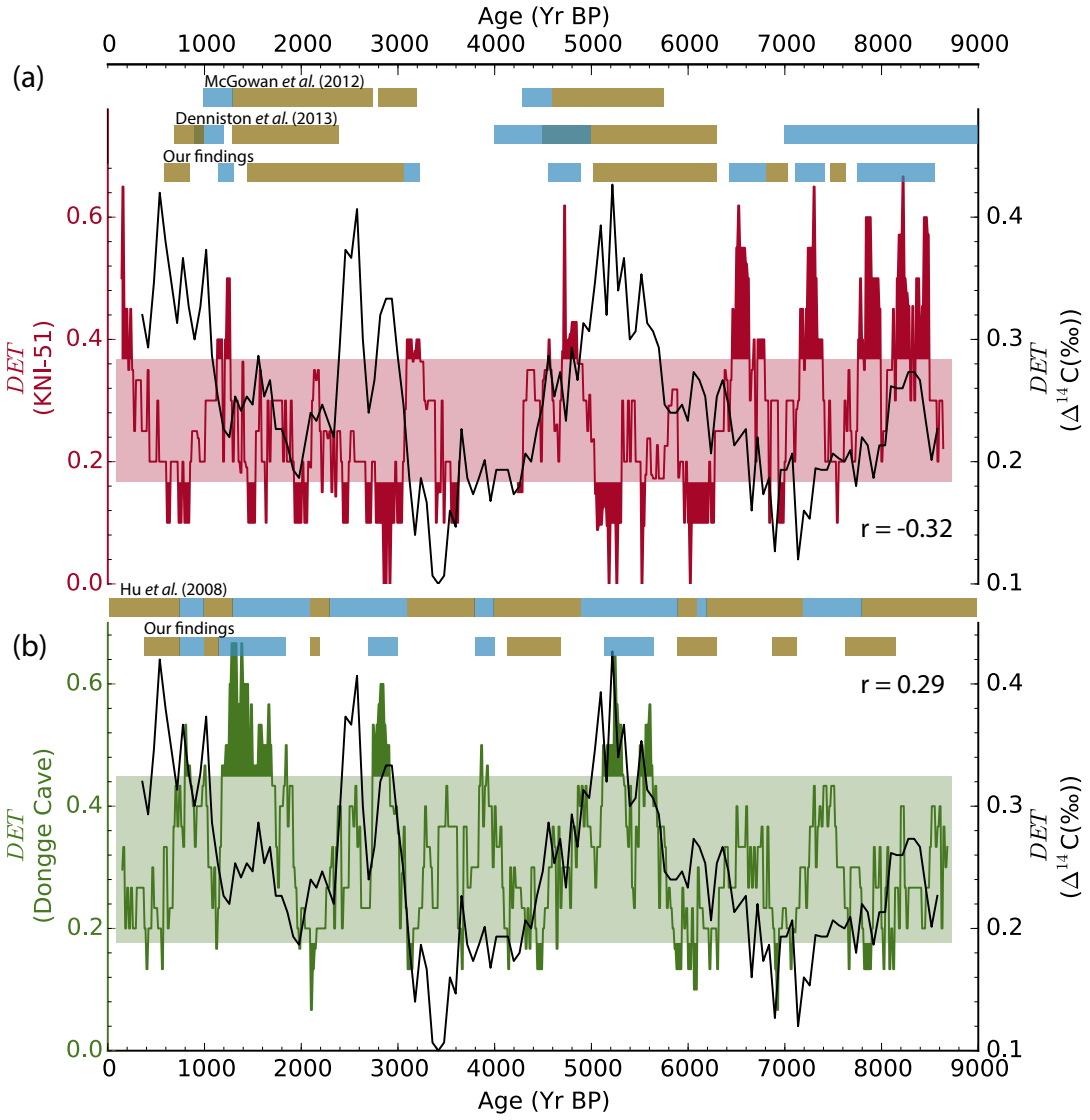

Figure 2: Determinism of the two proxy records (a) (red) KNI-51 and (b) (green) Dongge Cave. The determinism is calculated from the corresponding transformation costs time series and statistical significance is indicated by the two horizontal bands (see Supp. Mat. for details). High (low) determinism values correspond to wet (dry) monsoon regimes. The coloured bands (blue indicating wet regimes; brown, dry) provide a comparison of our findings with those of previous, qualitative studies. In the text we provide a detailed discussion of previously unidentified or incorrectly identified wet and dry regimes uncovered by our method. (black) Determinism of the solar activity proxy Δ^{14} C time series. Cross–correlation between the determinism of the solar activity proxy Δ^{14} C time series and KNI-51 time series is $r = -0.32$, and Dongge Cave time series is $r = 0.29$ (see Supp. Mat. for details).